

We are IntechOpen, the world's leading publisher of Open Access books Built by scientists, for scientists

6,900

Open access books available

185,000

International authors and editors

200M

Downloads

Our authors are among the

154

Countries delivered to

TOP 1%

most cited scientists

12.2%

Contributors from top 500 universities



WEB OF SCIENCE™

Selection of our books indexed in the Book Citation Index
in Web of Science™ Core Collection (BKCI)

Interested in publishing with us?
Contact book.department@intechopen.com

Numbers displayed above are based on latest data collected.
For more information visit www.intechopen.com



Cosmic Ray Muons as Penetrating Probes to Explore the World around Us

Paola La Rocca, Domenico Lo Presti and
Francesco Riggi

Additional information is available at the end of the chapter

<http://dx.doi.org/10.5772/intechopen.75426>

Abstract

Secondary cosmic muons provide a powerful probe to explore various aspects of the world around us. Various physical processes have been employed over the last years for such applications. Muon absorption was used to probe the interior of natural and man-made structures, from the Egypt pyramids to big volcanoes, contributing to interdisciplinary studies. Multiple scattering was employed to reconstruct the location of scattering centres, producing 2D and 3D images of the interior of hidden volumes (muon tomography). Additional possibilities of cosmic muons have been exploited even for the alignment of large civil structures and in the study of their stability. All these applications benefit from the development of advanced detection techniques and improvement in software algorithms. This contribution surveys the state of the art of these applications, with special emphasis on their possibilities and limitations.

Keywords: muon tomography, muon imaging, muon absorption, muon scattering, tracking detectors

1. Introduction

Since the early attempts to use cosmic muons as a probe to explore the inner part of solid structures [1], a variety of developments in muon tomography have been achieved, also exploiting new detection techniques and numerical algorithms for reconstruction and imaging. Correspondingly, the use of muons from the secondary cosmic radiation has found applications in many different fields, and an impressive list of documents, papers, projects related to such applications may be now easily found on the Web. From an historical point

of view, an important application of the muon absorption technique dates back to the work of Alvarez et al. [2], concerning the search for hidden chambers in one of the Egyptian pyramids. Nowadays, the applications of muon tomography to various aspects of everyday life include the study of large structures such as mountains and volcanoes, the inspection of large volumes to search for hidden, high-Z materials, such as for fissile illicit elements in containers, the monitoring of civil structures as large buildings or bridges, the control of nuclear reactors and their waste products, and many others.

It is usual to distinguish, from an experimental point of view, between those applications where the absorption of muons is employed to have information about the amount of material traversed by the particles and other applications where the multiple scattering effect is used instead, especially sensitive to the atomic number of the traversed material. Many examples of the two approaches have been given over the last two decades, and this review, although quoting many of these, is in no way a complete listing of what is available in the literature. Moreover, the field is rapidly expanding, with new detector prototypes being designed and tested, and many additional examples reported. After a brief introduction on the basic properties of the primary and secondary cosmic radiation, especially concerning the aspects which are relevant for muon tomography, a review of the problems and applications making use of the muon absorption technique is given in Section 3. Applications of the muon scattering are described in Section 4. Additional examples of applications of the muon interaction in matter are briefly reported in Section 5, while Section 6 reports a naïve discussion of the possible use of this technique outside our planet. Due to the importance of numerical algorithms for track reconstruction, and image processing, some of the relevant problems in this field are recalled in Section 7. Some concluding remarks are finally discussed in Section 8.

2. Basic properties of the primary and secondary cosmic radiation

Since its very beginning, our Earth is continuously bombarded by energetic particles—cosmic rays—which enter the Earth atmosphere from outer space. Most of them are charged nuclei, with H nuclei (protons) being dominant, and other, heavier nuclei, which reflect, with some difference, the nuclear abundance found in nature. Their energy may vary over many orders of magnitude, from a few hundred MeV to 10^{20} eV, with an energy spectrum roughly described by a power law, $dN/dE = \text{const } E^{-\gamma}$, with $\gamma = 2.7$ up to 3×10^{15} eV. At higher energies, up to 10^{19} eV, the spectrum steepens, with γ approximately equal to 3.1 (the so-called knee), flattening again above this energy. While a small fraction of the lowest energy particles come from our Sun, most of the primary cosmic rays originate from within the Milky Way, and the most energetic ones have an extra-galactic origin. Apart from the lowest energy component, which is subjected to space and time variations, due to the Sun and to the interplanetary environment, the majority of cosmic rays exhibit a homogeneous distribution, with very small anisotropies investigated, of the order of 10^{-4} to 10^{-3} .

The existence of the Earth atmosphere has a peculiar effect on the arrival of a primary cosmic ray, since an extensive air shower (EAS) is created following the first interaction

of a high energy primary particle with the atmospheric nuclei. This interaction produces a cascade of secondary particles, which may produce in turn additional particles or may decay, constituting a shower with hadronic and electromagnetic components. While a single detector may reveal the passage of individual particles in the shower, the coincidence detection between several particles in the shower allows the identification and reconstruction of the primary particle. This is the way in which extended arrays of detectors are able to measure even the largest energy primary particles. The lateral profile of extensive air showers depends on the initial energy and may reach hundreds of metres or even kilometres.

Apart from neutrinos, which are hardly detected, muons are the most penetrating part of the shower. Relativistic effects increase their lifetime (about 2.2 μ s at rest), allowing a large fraction of them to reach the Earth surface. Even though detailed measurements of the energy, angular distributions and charge ratio of cosmic muons at different altitudes and locations on the Earth surface are still pursued, especially for the high energy component, the basic properties of the muon flux are well known and many compilations exist concerning the distributions of these particles [3].

Several parameterizations exist for the angular and energy distributions of cosmic muons at the sea level or moderate altitudes. As a result of the muon absorption in the Earth atmosphere, the dependence on the zenithal angle θ at sea level is often expressed as

$$\frac{dN}{d\Omega} \sim \cos^2 \theta \quad (1)$$

while the momentum distribution of vertical muons roughly follows a power law. A reasonable parametrization of the vertical muon flux as a function of the momentum is given by [4].

$$C p^{-[c_0 + c_1 \ln p + c_2 (\ln p)^2 + c_3 (\ln p)^3]} \quad (2)$$

where the values of the c_i coefficients are given for selected ranges of the muon momentum. As an example, **Figure 1** shows a plot of the muon momentum distribution extracted from the above formula, for momenta up to about 1 TeV/c.

A semi-empirical parametrization of the muon flux at sea level as a function of both the zenithal angle and muon energy, especially valid for high energy muons ($E > 100$ GeV/cos θ) is the following:

$$\frac{dN}{dE d\Omega} = \frac{0.14 E^{-2.7}}{cm^2 s GeV sr} \left(\frac{1}{1 + \frac{1.1 E \cos \theta}{115 GeV}} + \frac{0.054}{1 + \frac{1.1 E \cos \theta}{850 GeV}} \right) \quad (3)$$

The mean energy of muons arriving at the sea level is ~ 4 GeV and the mean number of particles traversing a horizontal detector is of the order of 1 per cm² per minute. For detailed calculations one has to take into account the variations in these quantities which are due to the altitude and geographical location (especially latitude). On a large time scale, solar effects may also modify the numerical values of the measured flux.

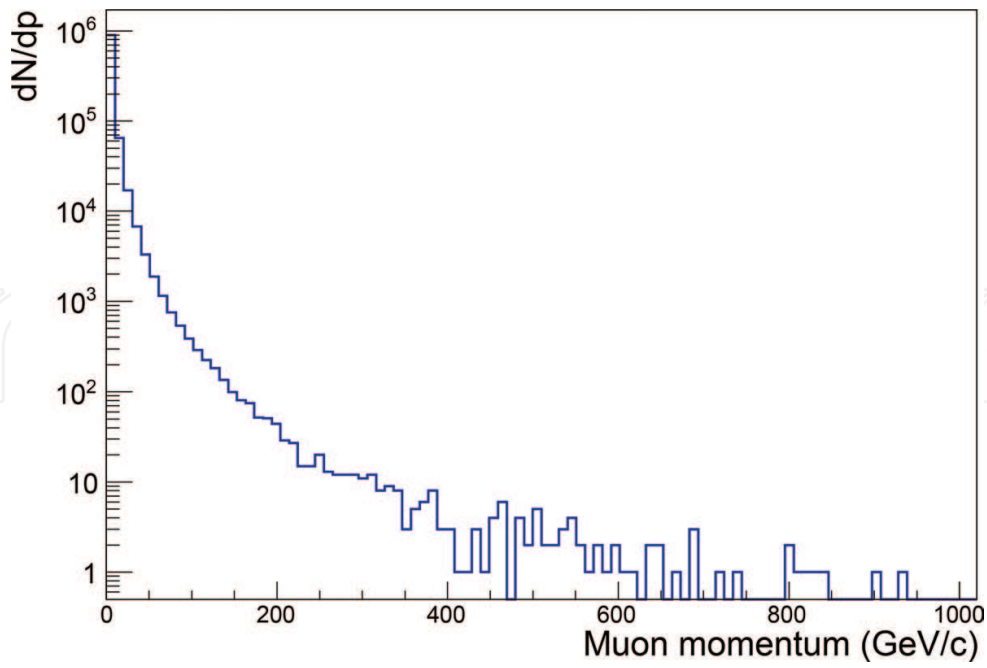


Figure 1. Momentum spectrum of cosmic muons, parametrized by Eq. (2).

3. Applications of the muon absorption technique

The exploration of heavy structures requires penetrating probes, in order to convey information concerning the interior of the structure and its details. For objects having sizes of the order of 1 m or less, X-rays or neutrons may constitute a valid alternative. For instance, typical mass attenuation coefficients of X-rays (30 keV) are of the order of $\mu/\rho = 30 \text{ cm}^2/\text{g}$ for Lead, so that a nonnegligible fraction of X-ray photons may penetrate several cm of Lead. **Figure 2** shows a plot of the mass attenuation coefficient for photons of various energies (from about 0.1 to 10 MeV) in Lead, as derived from the NIST standard data [5].

For larger size objects, the attenuation of such probes would be too high, and more penetrating particles, such as high energy muons, are required to traverse larger thicknesses. The basic properties of muon interaction in matter are known since a long time. However, their potential as a penetrating probe to give information on the interior of large structures is more recent, and only in the last years the literature has seen a large body of applications in this field, also related to the corresponding development of appropriate detectors, electronics, reconstruction and simulation algorithms.

The muon energy loss is usually expressed through its average value

$$-\frac{dE}{dx} = a(E) + b(E)E \quad (4)$$

where $a(E)$ takes into account the energy loss due to ionization, and $b(E)$ the energy loss due to other processes (e^+e^- pair production, Bremsstrahlung and photonuclear processes). The ionization term may be described by the Bethe-Bloch formula as a continuous process. At

very high muon energies however, radiative processes become more important than the ionization processes. In case of muons, the value of the critical energy, where the two contributions are comparable, is of the order of several hundred GeV for medium-Z materials like the Iron. Radiative processes then dominate the energy loss of highly energetic cosmic muons, and should be taken into account when considering muons which have to traverse hundred metres solid rock. As an example, **Figure 3** shows the muon energy loss in Lead as a function of the muon energy [6]. The relative contribution of the individual terms due to pair production, Bremsstrahlung and photonuclear processes depends on the muon energy, with the last one being much smaller than the other two for increasing muon energies.

Considering a realistic momentum distribution of muons, GEANT simulations of the interaction of muons with solid rock may be performed. As an example, **Figure 4** shows the fraction of surviving muons after traversing a given thickness of volcano rock, modelled by a realistic chemical composition of the lava from Etna, mainly including SiO_2 , Al_2O_3 , FeO , MgO , and CaO . As it is seen from **Figure 4**, about 1% of the muon flux is still emerging after traversing 100 m thickness.

Due to the energy loss of muons in a solid material (such as the rock of a mountain), which for a thin layer is proportional to the quantity ρdx , where ρ is the density of the material, the fraction of muons which survive after traversing a finite thickness x of material is given, to first order, by the integrated density over the path length L

$$\int_0^L \rho(x) dx \quad (5)$$

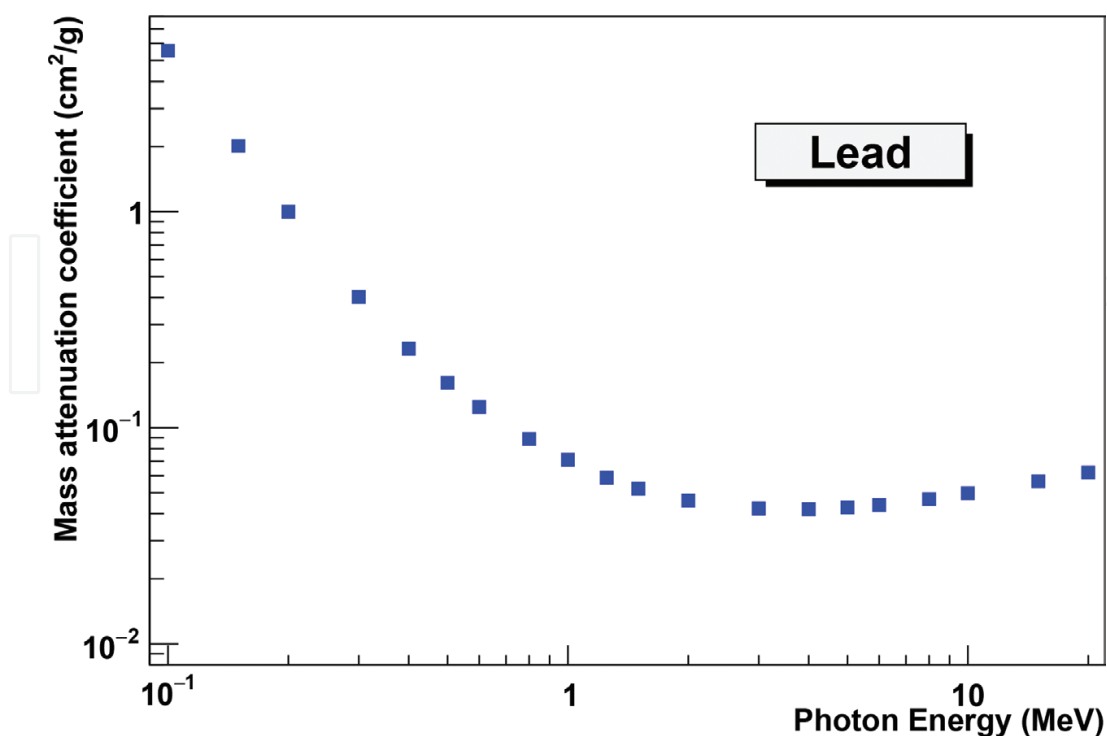


Figure 2. Mass attenuation coefficient of X- or γ -rays of various energies in lead, derived from the NIST standard data [5].

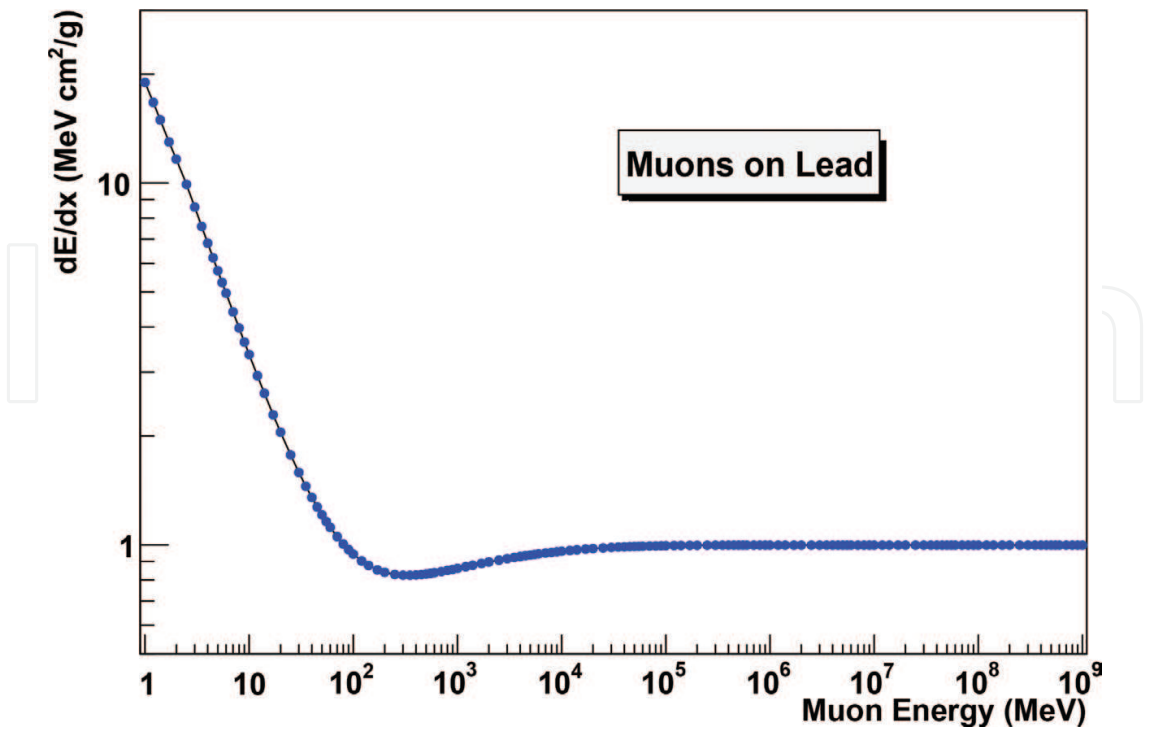


Figure 3. Muon energy loss in lead as a function of the muon energy, as derived from data reported in Ref. [6].

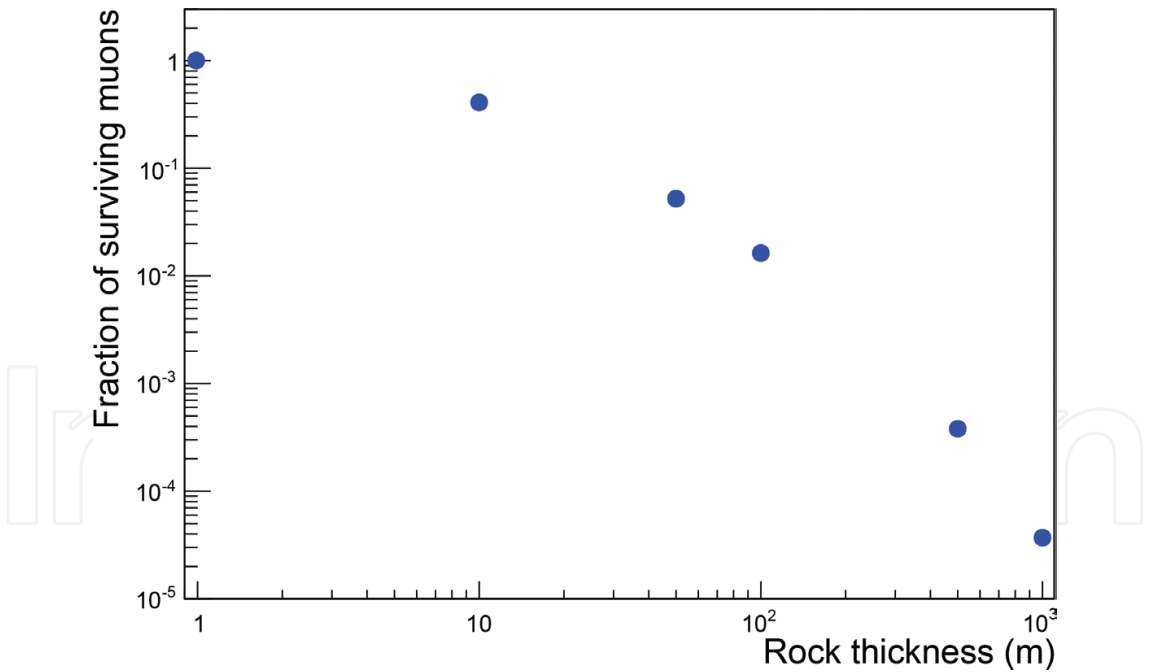


Figure 4. Transmission factor of cosmic muons as a function of the rock thickness traversed, as extracted from GEANT simulations for a realistic lava scenario from Mt. Etna.

Such quantity is sometimes called the opacity. A muon tracking detector, able to measure the number of muons arriving to it from any given direction, provides an experimental measurement of the opacity along different directions. The knowledge of the path length L for any

muon direction provides a density map, i.e. a map of the average density along that direction. A density map—once the actual traversed thickness is known and inserted for any specific orientation—may then reveal differences in the density evaluated along different directions. This is the basic principle of the muon absorption tomography. Although the muon absorption tomography may only provide two-dimensional density maps, in principle the combined use of several detectors, pointing to the object from different orientations may produce a 3D map of the object. The construction and use of a set of identical detectors, placed in different locations and working with comparable performance is not a trivial task and the real use of this opportunity is still to be exploited.

A standard setup for muon absorption experiments requires a muon tracking detector (telescope), usually employed in transmission mode (i.e. with the object being located between the open sky and the telescope). The reconstruction of a large number of tracks in the telescope allows for a 2D tomographic map, with a resolution which depends on the telescope tracking performance and on experimental disturbances such as multiple scattering effects in the material surrounding the object to be explored, as well as in the air. Many other aspects of the detector performance, such as its overall detection efficiency, response uniformity, sensitive area, alignment properties, duty cycle, cost and transportability, ... influence the real capability of the instrument.

Considering the possibilities offered by muon absorption tomography, several applications have been proposed, with many experimental results obtained so far. Here a brief review of these fields is given.

3.1. Vulcanology

A large interest in absorption muon tomography is related to the possibility of exploring the hidden part of mountains, especially active or potentially active volcanoes, by means of cosmic muons traversing part of their solid structure and being partially absorbed with respect to those coming from the open sky (**Figure 5**). This idea, exploited for the first time by Nagamine et al. in [7] and Tanaka et al. [8], has received an increasing attention in recent years, and a variety of projects, detector prototypes and operational activities have been reported. Important contributions to the field have been given by the Japanese collaboration led by H.K.M.Tanaka [8–12], which has employed a muon telescope made by several detection planes with scintillators with PMTs separated by Lead plates, by the Diaphane Collaboration [13–16], which carried out various measurement campaigns in several locations of the world (in France, Italy and Philippines) with scintillator-based muon telescopes, by the TOMUVOL Collaboration [17], employing resistive plate chambers detectors, and by the MU-RAY Project [18, 19], which has employed a muon telescope based on scintillator strips with SiPM photo-sensors for the exploration of Mt. Vesuvius in Italy.

A recent project has been developed also by our group in Catania, devoted to the study of the top craters of Mt. Etna, the highest active volcano in Europe, with a telescope equipped with three 1 m² segmented planes of scintillator strips with multianode PMT readout, already installed since last year close to the top of the mountain. Preliminary tomographic images of such craters have been already obtained by a comparison between the map produced by

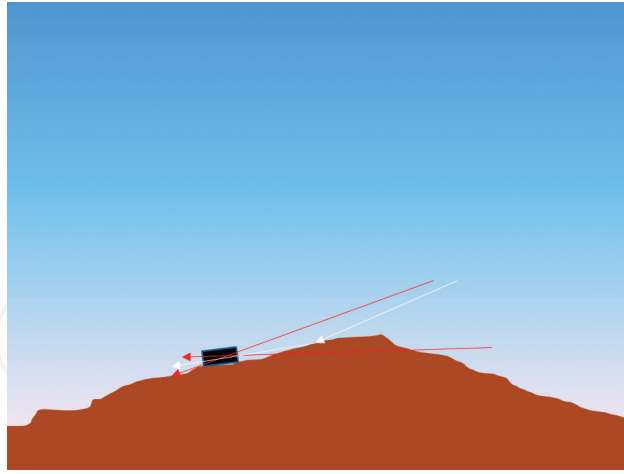


Figure 5. A simple geometrical sketch showing the principle of muon tomography applied to the study of mountain structures. A tracking telescope is placed downstream of the structure being explored, reconstructing muon tracks which ideally have traversed a thickness of solid rock. A comparison with the tracks coming from the open sky or from the backside is used to provide a 2D density map of the structure. A nonnegligible background however may originate from muons which are scattered either from the solid rock or from the air.

muons originating from the front side and the corresponding map produced by the muons coming from the back side.

It must be remembered that other Projects [20, 21] are exploiting the possibility to employ the Cerenkov light produced by the muons in the air after traversing the large thickness of the rock by a Cerenkov detector prototype (ASTRI), originally devised for astrophysical investigation in view of the large Cerenkov Telescope Array (CTA) Project.

The interest in this field is twofold: from one side methods based on muon tomography may complement and sometimes even surpass the potential offered by traditional methods in the understanding the inner part of these structures, revealing empty spaces, or different density profiles inside the mountain. On the other side there is the hope to reach the resolution and capability to monitor in real time the time evolution of the subsurface structures, in order to control potential activities giving rise to explosions and lava eruptions. This last possibility at the moment is still far from being fully reached, while static investigations have offered beautiful pictures of the interior of mountains and volcanoes in several parts of the world.

An important aspect of the technique, which in some cases offers a better figure of merit in comparison to geological and geophysics methods, is the spatial resolution, which can be expressed as

$$\Delta x = L \Delta \theta \quad (6)$$

where L is the distance between the detector and the structure being probed, and $\Delta \theta$ is the angular resolution of the tracking device. As an example, for a distance $L = 500$ m, and an angular resolution of $\Delta \theta = 1^\circ$, a spatial resolution of the order of 10 m is obtained, which is better than typical values of other geophysical methods.

3.2. Underground measurements

The use of absorption muon tomography is of course not only limited to the study of large mountain structures, but proves much more useful for the investigation of smaller geological locations, underground cavities, caverns, mines and tunnels, due to the reduced thickness to be explored, hence to the large flux being measured. There are several examples of the use of this technique for these applications [21–25]. As a recent example, in one of these investigations [22], carried out to explore underground cavities in the Naples area, a muon detector similar to that employed for volcano muography was employed, with size 1 m × 1 m, and segmented into 32 scintillator strips.

The vertical rock thickness above the detector was in the previous case about 40 m, which did not reduce too much the muon count rate, allowing for a significant result to be obtained in less than one month of data taking. Actually, for many of these applications, the range of rock thickness usually amounts to a few tens metres, which is a value much less than the values of interest for large volcanic structures. The possibility to install the detector in places which are not so prohibitive as for volcanic explorations gives larger opportunities to use this technique, which will likely be employed more and more in the near future to investigate underground environments.

3.3. Archaeology

As recalled at the beginning of this Chapter, one of the first examples of muon absorption tomography is represented by the well-known work by Alvarez and collaborators [2], who employed a muon detector inside an Egyptian pyramid to search for possible hidden chambers. The interest in the study of these very old structures is still very large, and in 2017 a recent study [26] was reported by the ScanPyramid Project, supported by many Institutions, who succeeded to find a very large (~ 30 m) unknown chamber in the Great or Khufu's Pyramid. Such void was first explored by nuclear emulsions and then confirmed by measurements carried out with scintillation hodoscopes and gas detectors; hence, it represents a beautiful example of interrelations between different observation techniques pointing to the same body of evidence. Additional examples of the use of the muon absorption technique for archaeological studies have been reported over the last years [27–29], among which is a study of the cavities in the Teotihuacan Pyramid of the Sun [27].

4. Muon scattering and tomography

The first investigation concerned with the use of the muon scattering process to obtain a radiography of the hidden content in a volume dates back to the work by Borozdin et al. [30], who employed a set of drift chambers (60 × 60 cm) to get radiographic images of tungsten blocks. This technique proved to be very promising for several reasons: it does not introduce any additional radiation, as it is for instance for X-rays; moreover, most of the scattered muons contribute to build the image, contrary to absorption, where a large fraction of muons is absorbed by the material itself. In the scattering mode, the muon tomography technique

makes use of this process, which strongly depends on the properties of the material, especially its atomic number Z , thus allowing to discriminate between low- and medium- Z elements with respect to high- Z elements.

The projected scattering angle distribution follows in a first approximation a Gaussian shape, with a width given by:

$$\theta_0 = \frac{13.6 \text{ MeV}}{\beta c p} \cdot Z \cdot \sqrt{\frac{x}{X_0}} \cdot \left[1 + 0.038 \ln \left(\frac{x}{X_0} \right) \right] \quad (7)$$

where p is the muon momentum, β is its speed, X the traversed thickness and X_0 the radiation length of the material, which in turn depends on the properties (Z , A) of the material roughly as

$$X_0 \approx \frac{\frac{716.4 \text{ g}}{\text{cm}^2}}{\rho} \frac{A}{Z(Z+1) \log \left(\frac{287}{\sqrt{Z}} \right)} \quad (8)$$

4.1. Homeland security

Due to the possibility that illicit fissile elements (Uranium or Plutonium) could be transported inside containers, this technique was suggested as a viable alternative to other traditional methods to inspect and scan a large volume. A muontomograph employing the scattering process basically requires two good muon tracking detectors, one placed above and the other placed below the volume to be inspected. Reconstruction of the muon track above and below the volume allows to evaluate the amount of scattering suffered by the muon, and in the simplest approach (where a single scattering centre is assumed), the so-called POCA (Point of Closest Approach) algorithm determines the 3D coordinates of the scattering centre (**Figure 6**). A sufficiently large number of individual tracks, traversing from any direction of the volume, allow to build 2D and 3D tomographic images. The performance of a muontomograph may be evaluated in terms of its spatial and angular resolution (depending on the tracking detectors), of the overall detection efficiency (which is the result of the detection efficiency of each tracking plane), which in turn determines the required scan time, of the capability to identify high- Z elements and discriminate them with respect to lighter elements, of the sensitivity to false-positive events, which would require an alarm and the opening of the container for a detailed control.

Several applications were oriented to the problem of scanning the content of a cargo container, searching for hidden high- Z materials, which is an important aspect of homeland security. Due to the large amount of containers travelling over the world, which is estimated to be larger than 200 M container/year, controlling the content of any of these volumes is a challenging task. At present, only a small fraction of them are checked, while laws under discussion might require more detailed procedures to be followed over the world. Following this approach, several small-scale prototypes have been built over the last years, employing a variety of detection technologies, from gas chambers to segmented strip scintillators,

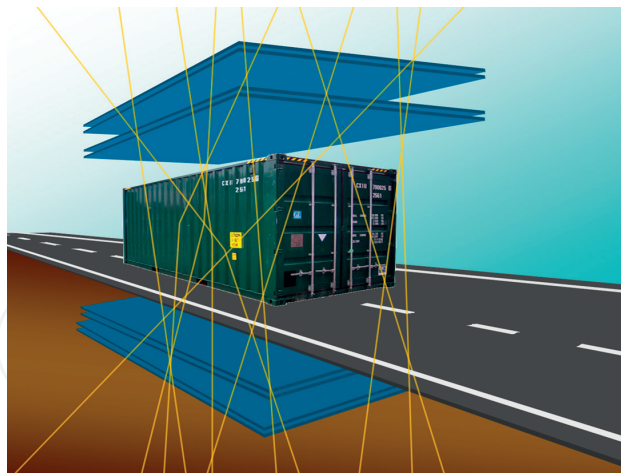


Figure 6. An artist view of the experimental setup being employed for muon tomography applications of cargo containers. Two muon tracking detectors, one placed above and the other placed below the container, are used to reconstruct muon tracks before and after traversing the container content.

Resistive Plate Chambers and GEM. Several contributions in this field have been reported by various groups [31–39], who have designed small scale as well as large and full-size scale detectors for muon tomography.

4.2. Nuclear reactors and waste imaging

For many decades, an impressive amount of used fuel has been produced, and most of this material is stored either in spent fuel pools or in dry storage casks. Such containers are sealed after filling them with the spent fuel, with no possibility to open and visually check their content. Monitoring nuclear waste is then an important aspect of the safety control in nuclear sites. Muon radiography, either in muon absorption or scattering mode, has proven to be a useful tool even for the exploration of nuclear waste storage silos, and many investigations have been already reported in this respect [40–45]. The integrity of nuclear reactors, especially after possible failures, is also a very demanding application for muon tomography [46–48] and following the Fukushima accident, it has been demonstrated that the muon scattering technique may be an answer to the problem of controlling the amount of material inside the reactor core [48].

Also the problem of detecting the presence of orphan sources in metal scraps container has received attention by muon tomography techniques [49, 50], since it is a potential source of large industrial accidents. Blast furnaces have been also explored by cosmic muons [51].

5. Other applications

In principle, dense structures may be explored by muon tomography, either by using the muon absorption or the scattering process, even if they are placed on the Earth surface. As an example, water towers were imaged by muon telescopes [52, 53], calibrating the response

of the detector as a function of the water content inside the tower. Post-injection monitoring of CO_2 stored in subsurface locations was investigated by several authors [54–56] by means of muon tomography. Industrial applications have also seen contribution from muon tomography [57, 58]. Finally, another application for the monitoring of civil buildings and structures which employs cosmic muons as a useful probe is the study of the angular distribution of muons detected in coincidence between a tracking detector on the ground and a set of additional detectors mechanically linked to the structure being monitored. Any movement of the structure with respect to the ground will result in a small modification of the distribution of the orientations of cosmic muons detected in coincidence, provided a good reconstruction of tracks and stable working conditions are achieved during long measurements [59, 60].

6. Muon tomography outside the Earth?

Since cosmic rays originate from any direction and permeate all the known Universe, the question whether the same concepts discussed so far apply also to other places outside our terrestrial environment is intriguing. Limiting ourselves to the nearest environment outside the Earth, namely the Solar System, the interaction of the primary cosmics with other planets and celestial bodies produces different results depending on the presence of an atmosphere around the solid structure of the body. For planets or satellites where no atmosphere at all exists, such for instance the Moon, energetic primary particles interact with the surface without producing an extensive air shower. In other situations, where a massive atmosphere exists, much deeper and dense than the Earth atmosphere, as for instance on Venus or Jupiter, air showers may be created but most of the secondary particles are subsequently absorbed by the atmosphere itself, so that only a very small fraction of particles is able to arrive to the surface. Monte Carlo calculations of the interaction of energetic particles with the detailed structure of these bodies should be carried out for any specific situation in order to understand their peculiarities. In case of Mars, where the atmospheric pressure near the surface is only 1/100 with respect to Earth, the development of air showers has been studied in some detail by Tanaka [61], allowing to understand how the proportion between primary protons and secondary pions or muons is very much different than on Earth. In particular, due to the reduced thickness of the Martian atmosphere, the vertical flux of muons is much smaller with respect to the values obtained on the Earth; however, for inclined muons, close to the horizontal, the situation is reversed, and a larger flux of muons would be observed. In any case, contamination from the primary protons is a challenge, and some way to discriminate between the two species should be devised. It is interesting that such concepts have been discussed with relation to realistic Martian exploration missions, trying to understand even the practical aspects and problems which would be required to solve to carry out tomographic measurements on the Red Planet [62, 63].

7. Imaging and simulation methods and algorithms

Muon tomography has offered over the last years also a good environment for the development of mathematical and statistical algorithms, numerical simulation and procedures, to

understand and analyze the experimental data being collected, improve the reconstruction and imaging techniques and help to design new apparatus and evaluate their performance.

One of the items that has been long discussed in the muon scattering technique is the reconstruction of the distribution of the scattering centres, leading to a 2D or 3D tomographic image. While the simplest approach employs the POCA method, as discussed in Section 4, better algorithms and methods have been introduced, especially to deal with situations where multiple scattering centres exist. The Maximum Likelihood/Expectation Maximization (EL/EM) iterative method [64] is employed as a valid alternative for processing muon scattering data and reconstruct tomographic images.

Clustering algorithms, which are a set of multivariate data analysis techniques, have been also used to group homogeneous items in a dataset. One of the most known clustering algorithms is the Friends-of-Friends. Applied to muon tomography, clustering analysis helps to detect objects within a spatial domain [65].

Another important aspect of the development of numerical methods in muon tomography is concerned with physics simulations. The importance of numerical simulations in the design of an experimental setup, as well as in the correct interpretation of the effects observed, has been long recognized in nuclear and particle physics and it is nowadays a routine aspect of any quantitative experimental investigation. This is also the case for any tomographic study carried out with cosmic muons. Very frequently, reconstruction and imaging algorithms are tested against simulated data, to compare the merits of different approaches and evaluate their inherent performance. In other cases, only a detailed simulation of the physics processes taking place in the experimental setup and in the surrounding environment may help to understand important aspects of the problem. As an example, the study of the background contribution to the direct flux of muons arriving to the detector through the rock is very important, since in some cases this contribution may be even larger than the direct flux [66], thus leading to an overestimation. In many cases a detailed simulation of the initial energy and angular cosmic particle distributions, coupled to a transport study of these particles along the mountain profile may help to disentangle some of these aspects and provide a quantitative estimate of the role of the background in the corresponding measurements.

8. Conclusions

The list of possible applications provided by this short review is not at all exhaustive, and many other examples of the use of cosmic-ray muons to explore various aspects of our environment are available in the literature [67]. Since the first quantitative investigations at the end of 1990s, in about 20 years, the use of cosmic-ray muons for imaging has grown in interest and this technique is now enough consolidated to be proposed even for commercial use. The variety of possible applications in the field has promoted interdisciplinary studies, with the contribution of experts from different areas, and has already given interesting results in many practical situations. The number of papers, articles, technical reports and conference contributions is more and more large, and specialized conferences and workshop have been organized in the last few years to promote exchange of opinions and results, new collaborations and

efforts. Even though many promising results have been reported in various fields of interest, there is still a wide territory where to improve the existing techniques. One important aspect is the detection technology, which has been object of several possible choices, and it is still a point of discussion in terms of the optimization of the performance (especially efficiency and resolution) and cost. Also the existing algorithms and methods may be largely improved to arrive to a better reconstruction and imaging processing of experimental data. The years to come are then a promising period for the development of all such aspects, in view of new applications, only limited by the creativity of interested people, or of large improvements in the existing ones.

Acknowledgements

The authors gratefully acknowledge the fruitful collaboration with many colleagues, students and technicians of the Department of Physics and Astronomy of the University of Catania, of the National Institute for Nuclear Physics (INFN) and National Institute for Astrophysics (INAF), while carrying out various projects concerned with muon tomography.

Author details

Paola La Rocca, Domenico Lo Presti and Francesco Riggi*

*Address all correspondence to: Francesco.Riggi@ct.infn.it

Department of Physics and Astronomy, University of Catania, Catania, Italy

References

- [1] George EP. Cosmic rays measure overburden of tunnel. *Commonwealth Engineer*. 1955;455-457
- [2] Alvarez LW et al. Search for hidden chambers in the pyramids. *Science*. 1970;**167**:832-839. DOI: 10.1126/science.167.3919.832
- [3] See e.g. Grieder PKF. *Cosmic Rays at Earth*. 1st ed. Amsterdam: Elsevier Science; 2001. 1112 p. ISBN: 9780444507105
- [4] Bugaev EV et al. Atmospheric muon flux at sea level, underground and underwater. *Physical Review D*. 1998;**58**:054001. DOI: 10.1103/PhysRevD.58.054001
- [5] National Institute of Standards and Technology. <https://www.nist.gov/>
- [6] Data taken from <http://pdg.lbl.gov/AtomicNuclearProperties/>
- [7] Nagamine K et al. Method of probing inner structure of geophysical substance with the horizontal cosmic ray muons and possible application to volcanic eruption prediction. *Nuclear Instruments and Methods A*. 1995;**356**:585-595. DOI: 10.1016/0168-9002(94)01169-9

- [8] Tanaka HKM et al. Development of the cosmic-ray muon detection system for probing the internal structure of a volcano. *Hyperfine Interactions*. 2001;**138**:521-526. DOI: 10.1023/A:1020843100008
- [9] Tanaka HKM et al. Radiographic visualization of magma dynamics in an erupting volcano. *Nature Communications*. 2014;**5**:3381. DOI: 10.1038/ncomms4381
- [10] Tanaka HKM. Visualization of the internal structure of volcanoes with cosmic-ray muons. *Journal of the Physical Society of Japan*. 2016;**85**:091016. DOI: 10.7566/JPSJ.85.091016
- [11] Tanaka HKM. Instant snapshot of the internal structure of Unzen lava dome, Japan with airborne muography. *Scientific Reports*. 2016;**6**:39741. DOI: 10.1038/srep39741
- [12] Kusagaya T, Tanaka HKM. Muographic imaging with a multi-layered telescope and its application to the study of the subsurface structure of a volcano. *Proceedings of the Japan Academy, Series B, Physical and Biological Sciences*. 2015;**91**:501-510. DOI: 10.2183/pjab.91.501
- [13] Gibert D et al. Muon tomography: Plans for observations in the lesser Antilles. *Earth, Planets and Space*. 2010;**62**:153-165. DOI: 10.5047/eps.2009.07.003
- [14] Lesparre N et al. Geophysical muon imaging: Feasibility and limits. *Geophysical Journal International*. 2010;**183**:1348-1361. DOI: 10.1111/j.1365-246X.2010.04790.x
- [15] Marteau J et al. Muons tomography applied to geosciences and volcanology. *Nuclear Instruments and Methods A*. 2012;**695**:23. DOI: 10.1016/j.nima.2011.11.061
- [16] Carbone D et al. An experiment of muon radiography at Mt Etna (Italy). *Geophysical Journal International*. 2014;**196**:633-643. DOI: 10.1093/gji/ggt403
- [17] Carloganu C. Density imaging of volcanoes with atmospheric Muons using GRPCs. In: *Proceedings of Science 055 (POS EPS-HEP2011)*. 2011
- [18] Ambrosi G et al. The MU-RAY project: Volcano radiography with cosmic-ray muons. *Nuclear Instruments and Methods A*. 2011;**628**:120-123. DOI: 10.1016/j.nima.2010.06.299
- [19] Ambrosino F et al. The MU-RAY project: Detector technology and first data from Mt. Vesuvius or silicon detectors. *Journal of Instrumentation*. 2014;**9**:C02029. DOI: 10.1088/1748-0221/9/02/C02029
- [20] Catalano O et al. Volcanoes muon imaging using Cherenkov telescopes. *Nuclear Instruments and Methods A*. 2016;**807**:5-12. DOI: 10.1016/j.nima.2015.10.065
- [21] Del Santo M et al. Looking inside volcanoes with the imaging atmospheric Cherenkov telescopes. *Nuclear Instruments and Methods A*. 2017;**876**:111-114. DOI: 10.1016/j.nima.2017.02.029
- [22] Caffau E et al. Underground cosmic-ray measurement for morphological reconstruction of the Grotta Gigante natural cave. *Nuclear Instruments and Methods A*. 1997;**385**:480-488. DOI: 10.1016/S0168-9002(96)01041-8

- [23] Saracino G et al. Imaging of underground cavities with cosmic-ray muons from observations at Mt. Echia (Naples). *Nature Scientific Reports*. 2017;**7**:1181. DOI: 10.1038/s41598-017-01277-3
- [24] Malmqvist L et al. Theoretical studies of *in-situ* rock density determinations using underground cosmic-ray muon intensity measurements with application in mining geophysics. *Geophysics*. 1979;**44**:1549. DOI: 10.1190/1.1441026
- [25] Fujii H et al. Detection of on-surface objects with an underground radiography detector system using cosmic-ray muons. *Progress of Theoretical and Experimental Physics*. 2017;**5**:053C01. DOI: 10.1093/ptep/ptx061
- [26] Barnafoldi GG et al. Portable cosmic muon telescope for environmental applications. *Nuclear Instruments and Methods A*. 2012;**689**:60-69. DOI: 10.1016/j.nima.2012.06.015
- [27] Morishima K et al. Discovery of a big void in Khufu's pyramid by observation of cosmic-ray muons. *Nature*. 2017;**552**:386-390. DOI: 10.1038/nature24647
- [28] Menchaca-Rocha A. Searching for cavities in the Teotihuacan Pyramid of the Sun using cosmic muons experiments and instrumentation. In: *Proceedings of the 32nd International Cosmic Ray Conference (ICRC2011)*; 11-18 August 2011; Beijing, China. 2011;**4**:325-328. DOI: 10.7529/ICRC2011/V04/1117
- [29] Gómez H et al. Studies in muon tomography for archaeological internal structures scanning. *Journal of Physics Conference Series*. 2016;**718**:052016. DOI: 10.1088/1742-6596/718/5/052016
- [30] Gómez H et al. Feasibility study of archaeological structures scanning by muon tomography. *AIP Conference Proceedings*. 2015;**1672**:140004. DOI: 10.1063/1.4928020
- [31] Borozdin KN et al. Radiographic imaging with cosmic-ray muons. *Nature*. 2003;**422**:277. DOI: 10.1038/422277a
- [32] Schultz LJ et al. Image reconstruction and material Z discrimination via cosmic ray muon radiography. *Nuclear Instruments and Methods A*. 2004;**519**:687-694. DOI: 10.1016/j.nima.2003.11.035
- [33] Gnanvo K et al. Imaging of high-Z material for nuclear contraband detection with a minimal prototype of a muon tomography station based on GEM detectors. *Nuclear Instruments and Methods A*. 2011;**652**:16-20. DOI: 10.1016/j.nima.2011.01.163
- [34] Baesso P et al. Towards a RPC-based muon tomography system for cargo containers. *Journal of Instrumentation*. 2014;**9**:C10041. DOI: 10.1088/1748-0221/9/10/C10041
- [35] Pesente S et al. First results on material identification and imaging with a large volume muon tomography prototype. *Nuclear Instruments and Methods A*. 2009;**604**:738-746. DOI: 10.1016/j.nima.2009.03.017
- [36] Anghel V et al. A plastic scintillator-based muon tomography system with an integrated muon spectrometer. *Nuclear Instruments and Methods A*. 2015;**789**:12-23. DOI: 10.1016/j.nima.2015.06.054

- [37] Riggi S et al. A large area cosmic ray detector for the inspection of hidden high-Z materials inside containers. *Journal of Physics: Conference Series*. 2013;**409**:012046. DOI: 10.1088/1742-6596/409/1/012046
- [38] Riggi F et al. The Muon portal project: A large-area tracking detector for muon tomography. *EPJ Web of Conferences*. 2016;**117**:05003. DOI: 10.1051/epjconf/201611705003
- [39] Antonuccio V et al. The Muon portal project: Design and construction of a scanning portal based on muon tomography. *Nuclear Instruments and Methods A*. 2017;**845**:322-325. DOI: 10.1016/j.nima.2016.05.006
- [40] Wang X et al. The cosmic ray muon tomography facility based on large scale MRPC detectors. *Nuclear Instruments and Methods A*. 2015;**784**:390-393. DOI: 10.1016/j.nima.2015.01.024
- [41] Clarkson A et al. Characterising encapsulated nuclear waste using cosmic-ray muon tomography. *Journal of Instrumentation*. 2015;**10**:P03020. DOI: 10.1088/1748-0221/10/03/P03020
- [42] Clarkson A et al. The design and performance of a scintillating-fibre tracker for the cosmic-ray Muon tomography of legacy nuclear waste containers. *Nuclear Instruments and Methods A*. 2014;**745**:138-149. DOI: 10.1016/j.nima.2014.01.062
- [43] Poulson D et al. Cosmic ray muon computed tomography of spent nuclear fuel in dry storage casks. *Nuclear Instruments and Methods A*. 2017;**842**:48-53. DOI: 10.1016/j.nima.2016.10.040
- [44] Chatzidakis S et al. Interaction of cosmic ray muons with spent nuclear fuel dry casks and determination of lower detection limit. *Nuclear Instruments and Methods A*. 2016;**828**:37-45. DOI: 10.1016/j.nima.2016.03.084
- [45] Jonkmans G et al. Nuclear waste imaging and spent fuel verification by muon tomography. *Annals of Nuclear Energy*. 2013;**53**:267-273. DOI: 10.1016/j.anucene.2012.09.011
- [46] Ambrosino F et al. Assessing the feasibility of interrogating nuclear waste storage silos using cosmic-ray muons. *Journal of Instrumentation*. 2015;**10**:T06005. DOI: 10.1088/1748-0221/10/06/T06005
- [47] Fujii H et al. Performance of a remotely located muon radiography system to identify the inner structure of a nuclear plant. *Progress of Theoretical and Experimental Physics*. 2013;**7**:073C01. DOI: 10.1093/ptep/ptt046
- [48] Perry J et al. Imaging a nuclear reactor using cosmic ray muons. *Journal of Applied Physics*. 2013;**113**:184909. DOI: 10.1063/1.4804660
- [49] Borozdin K et al. Cosmic ray radiography of the damaged cores of the Fukushima reactors. *Physical Review Letters*. 2012;**109**:152501. DOI: 10.1103/PhysRevLett.109.152501
- [50] Bonomi G et al. Muon tomography as a tool to detect radioactive source shielding in scrap metal containers. *International Journal of Modern Physics: Conference Series*. 2014;**27**:1460157. DOI: 10.1142/S2010194514601574

- [51] Furlan M et al. Application of muon tomography to detect radioactive sources hidden in scrap metal containers. *IEEE Transaction on Nuclear Science*. 2014;**61**:2204. DOI: 10.1109/ANIMMA.2013.6728043
- [52] Nagamine K et al. Probing the inner structure of blast furnaces by cosmic-ray muon radiography. *Proceedings of the Japan Academy, Series B*. 2005;**81**:257-260. DOI: 10.2183/pjab.81.257
- [53] Bouteille S et al. A Micromegas-based telescope for muon tomography: The WatTo experiment. *Nuclear Instruments and Methods A*. 2016;**834**:223-228. DOI:10.1016/j.nima.2016.08.002
- [54] Jourde K et al. Monitoring temporal opacity fluctuations of large structures with muon tomography: A calibration experiment using a water tower tank. *Scientific Reports*. 2016;**6**:23054. DOI: 10.1038/srep23054
- [55] Kudryvtsev A et al. Monitoring subsurface CO₂ injection and security of storage using muon tomography. *International Journal of Greenhouse Gas Control*. 2012;**11**:21-24. DOI: 10.1016/j.ijggc.2012.07.023
- [56] Klinger J et al. Simulation of muon radiography for monitoring CO₂ stored in a geological reservoir. *International Journal of Greenhouse Gas Control*. 2015;**42**:644
- [57] Pal S et al. Muon tomography for carbon storage and monitoring. In: Bhuyan B, editors. *XXI DAE-BRNS High Energy Physics Symposium*. Springer Proceedings in Physics, Vol. 174; 2016. pp. 479-485. DOI: 10.1007/978-3-319-25619-1_73
- [58] Gilboy WB et al. Industrial thickness gauging with cosmic-ray muons. *Radiation Physics and Chemistry*. 2005;**74**:454-458. DOI: 10.1016/j.radphyschem.2005.08.007
- [59] Durham JM et al. Tests of cosmic ray radiography for power industry applications. *AIP Advances*. 2015;**5**:067111. DOI: 10.1063/1.4922006
- [60] Bodini I et al. Cosmic ray detection based measurement systems. *Measurement Science and Technology*. 2007;**18**:3537. DOI: 10.1088/0957-0233/18/11/038
- [61] Donzella A et al. Historical building stability monitoring by means of a cosmic ray tracking system. *NuovoCimento C*. 2014;**37**:223-232. DOI: 10.1393/ncc/i2014-11806-3
- [62] Tanaka H. Monte-Carlo simulations of atmospheric muon production: Implication of the past martian environment. *Icarus*. 2007;**19**:603-615. DOI: 10.1016/j.icarus.2007.05.014
- [63] Kedar S et al. Low cost, low power, passive muon telescope for interrogating martian subsurface. *Concepts and Approach for Mars Exploration*. 2012;**1679**:4150
- [64] Kedar S et al. Muon radiography for exploration of Mars geology. *Geoscientific Instrumentation, Methods and Data Systems*. 2013;**2**:157-164. DOI: 10.5194/gi-2-157-2013
- [65] Schultz LJ et al. Statistical reconstruction for cosmic ray muon tomography. *IEEE Transactions on Image Processing*. 2007;**16**:1985-1993. DOI: 10.1109/TIP.2007.901239

- [66] Bandieramonte M et al. Clustering analysis for muon tomography data elaboration in the muon portal project. *Journal of Physics Conference Series*. 2015;**608**:012046. DOI: 10.1088/1742-6596/608/1/012046
- [67] Nishiyama R et al. Monte Carlo simulation for background study of geophysical inspection with cosmic-ray muons. *Geophysical Journal International*. 2016;**206**:1039-1050. DOI: 10.1093/gji/ggw191

